CEP128 Localizes to the Subdistal Appendages of the Mother Centriole and Regulates TGF-/BMP Signaling at the Primary Cilium

Mönnich, Maren; Borgeskov, Louise; Breslin, Loretta; Jakobsen, Lis; Rogowski, Michaela; Doganli, Canan; Schrøder, Jacob M; Mogensen, Johanne B; Blinkenkjær, Louise; Harder, Lea M; Lundberg, Emma; Geimer, Stefan; Christensen, Søren T; Andersen, Jens S.; Larsen, Lars A; Pedersen, Lotte B

Published in:
Cell Reports

DOI:
10.1016/j.celrep.2018.02.043

Publication date:
2018

Document version
Publisher's PDF, also known as Version of record

Report

Cell Reports

CEP128 Localizes to the Subdistal Appendages of the Mother Centriole and Regulates TGF-β/BMP Signaling at the Primary Cilium

Graphical Abstract

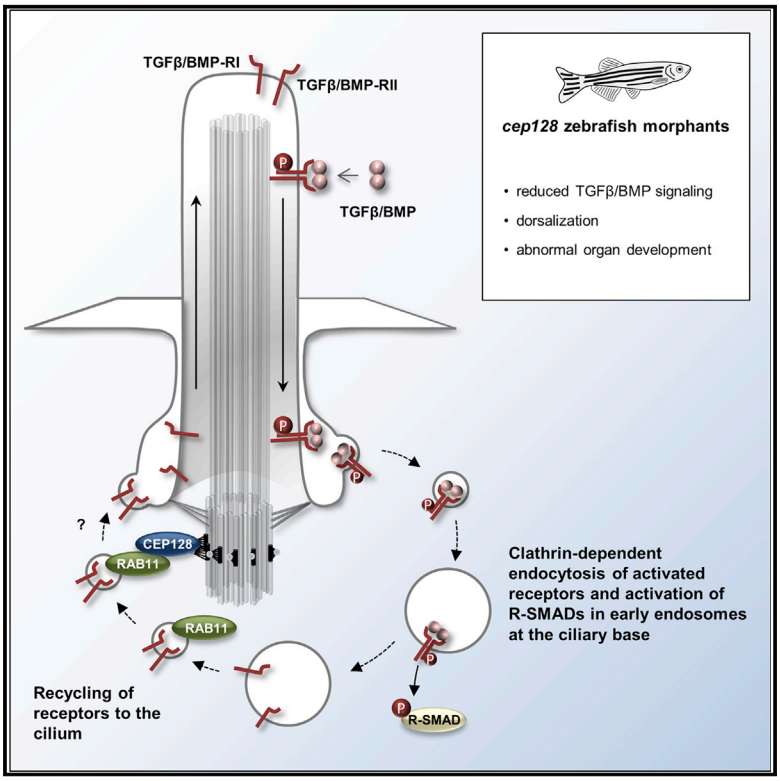

Highlights

- CEP128 localizes to the subdistal appendages of the mother centriole and basal body
- *cep128* zebrafish morphants display impaired TGF-β/BMP signaling and organ development
- CEP128 loss in mammalian cells leads to reduced TGF-β/BMP signaling at the primary cilium
- Impaired signaling is linked to defective vesicular trafficking and ciliary loss of RAB11

Authors

Maren Mönnich, Louise Borgeskov, Loretta Breslin, ..., Jens S. Andersen, Lars A. Larsen, Lotte B. Pedersen

Correspondence

stefan.geimer@uni-bayreuth.de (S.G.), stchristensen@bio.ku.dk (S.T.C.), jens.andersen@bmb.sdu.dk (J.S.A.), larsal@sund.ku.dk (L.A.L.), lbpedersen@bio.ku.dk (L.B.P.)

In Brief

Mönnich et al. show that CEP128 localizes to the subdistal appendages of the mother centriole and basal body of the primary cilium. CEP128 regulates vesicular trafficking and targeting of RAB11 to the primary cilium. CEP128 loss leads to impaired TGF-β/BMP signaling, which, in zebrafish, is associated with defective organ development.

Mönnich et al., 2018, Cell Reports *22*, 2584–2592
March 6, 2018
https://doi.org/10.1016/j.celrep.2018.02.043

CellPress

OPEN ACCESS
CellPress

Cell Reports
Report

CEP128 Localizes to the Subdistal Appendages of the Mother Centriole and Regulates TGF-β/BMP Signaling at the Primary Cilium

Maren Mönnich,[1,6] Louise Borgeskov,[2,6] Loretta Breslin,[2,3,6] Lis Jakobsen,[3,6] Michaela Rogowski,[4] Canan Doganli,[1] Jacob M. Schrøder,[3] Johanne B. Mogensen,[2] Louise Blinkenkjær,[2] Lea M. Harder,[3] Emma Lundberg,[5] Stefan Geimer,[4,*] Søren T. Christensen,[2,*] Jens S. Andersen,[3,*] Lars A. Larsen,[1,*] and Lotte B. Pedersen[2,7,*]

[1]Department of Cellular and Molecular Medicine, University of Copenhagen, DK-2200 Copenhagen, Denmark
[2]Department of Biology, University of Copenhagen, DK-2100 Copenhagen, Denmark
[3]Department of Biochemistry and Molecular Biology, University of Southern Denmark, Campusvej 55, DK-5230 Odense M, Denmark
[4]Cell Biology/Electron Microscopy, University of Bayreuth, Universitaetsstrasse 30, 95440 Bayreuth, Germany
[5]Science for Life Laboratory, School of Biotechnology, KTH Royal Institute of Technology, SE-171 21 Stockholm, Sweden
[6]These authors contributed equally
[7]Lead Contact
*Correspondence: stefan.geimer@uni-bayreuth.de (S.G.), stchristensen@bio.ku.dk (S.T.C.), jens.andersen@bmb.sdu.dk (J.S.A.), larsal@sund.ku.dk (L.A.L.), lbpedersen@bio.ku.dk (L.B.P.)
https://doi.org/10.1016/j.celrep.2018.02.043

SUMMARY

The centrosome is the main microtubule-organizing center in animal cells and comprises a mother and daughter centriole surrounded by pericentriolar material. During formation of primary cilia, the mother centriole transforms into a basal body that templates the ciliary axoneme. Ciliogenesis depends on mother centriole-specific distal appendages, whereas the role of subdistal appendages in ciliary function is unclear. Here, we identify CEP128 as a centriole subdistal appendage protein required for regulating ciliary signaling. Loss of CEP128 did not grossly affect centrosomal or ciliary structure but caused impaired transforming growth factor-β/bone morphogenetic protein (TGF-β/BMP) signaling in zebrafish and at the primary cilium in cultured mammalian cells. This phenotype is likely the result of defective vesicle trafficking at the cilium as ciliary localization of RAB11 was impaired upon loss of CEP128, and quantitative phosphoproteomics revealed that CEP128 loss affects TGF-β1-induced phosphorylation of multiple proteins that regulate cilium-associated vesicle trafficking.

INTRODUCTION

Primary cilia are surface-exposed sensory organelles that coordinate important cellular and developmental signaling pathways in vertebrates, including Hedgehog (Huangfu et al., 2003) and transforming growth factor (TGF)-β signaling (Clement et al., 2013). Structural or functional defects in cilia, therefore, lead to diseases, ciliopathies, which affect many different organs and tissues in the body (Kenny and Beales, 2014).

Primary cilia contain a 9+0 microtubule (MT) axoneme that extends from a basal body and is surrounded by a bilayer lipid membrane enriched for specific receptors and ion channels. The transition zone at the ciliary base, functioning as a selective gate, ensures that the organelle has a unique protein and lipid composition compared to the cell body (Jensen and Leroux, 2017). Intraflagellar transport (IFT) also contributes to this compartmentalization and mediates assembly and maintenance of the ciliary axoneme (Taschner and Lorentzen, 2016).

Ciliogenesis begins in G_1/G_0 with the docking of vesicles to the mother centriole distal end (Sorokin, 1962), which contains distal and subdistal appendages with distinct composition and functions. Distal appendage proteins (DAPs) promote ciliogenesis by providing vesicle and IFT docking sites (Wei et al., 2015; Deane et al., 2001), whereas the role of subdistal appendage proteins (SDAPs) in ciliary assembly and function is unclear. The SDAPs ninein, cenexin1 (an ODF2 splice variant), CNTRL, and CC2D2A were reported to promote ciliogenesis (Graser et al., 2007; Hehnly et al., 2012; Veleri et al., 2014; Hung et al., 2016), whereas other researchers have questioned the role of SDAPs in this process (Tateishi et al., 2013; Mazo et al., 2016). In addition, SDAPs were implicated in MT anchoring (Mogensen et al., 2000; Guarguaglini et al., 2005), regulating vesicle trafficking (Gromley et al., 2005; Hehnly et al., 2012; Hung et al., 2016), linking the centrosome to the Golgi (Mazo et al., 2016), and promoting basal body alignment in multiciliated cells (Kunimoto et al., 2012; Clare et al., 2014).

Here, we identify CEP128 as an SDAP that regulates TGF-β/bone morphogenetic protein (BMP) signaling and RAB11 trafficking at the primary cilium. By gene silencing or knockout in cultured mammalian cells, we find that lack of CEP128 has no major effect on centrosome structure but leads to increased ciliation frequency, as reported previously (Gupta et al., 2015). Depletion of *cep128* in zebrafish caused severe developmental defects reminiscent of defective TGF-β/BMP signaling, as well as reduced phosphorylation of Smad1/2/5/8. Mammalian cell culture assays and quantitative phosphoproteomics analysis

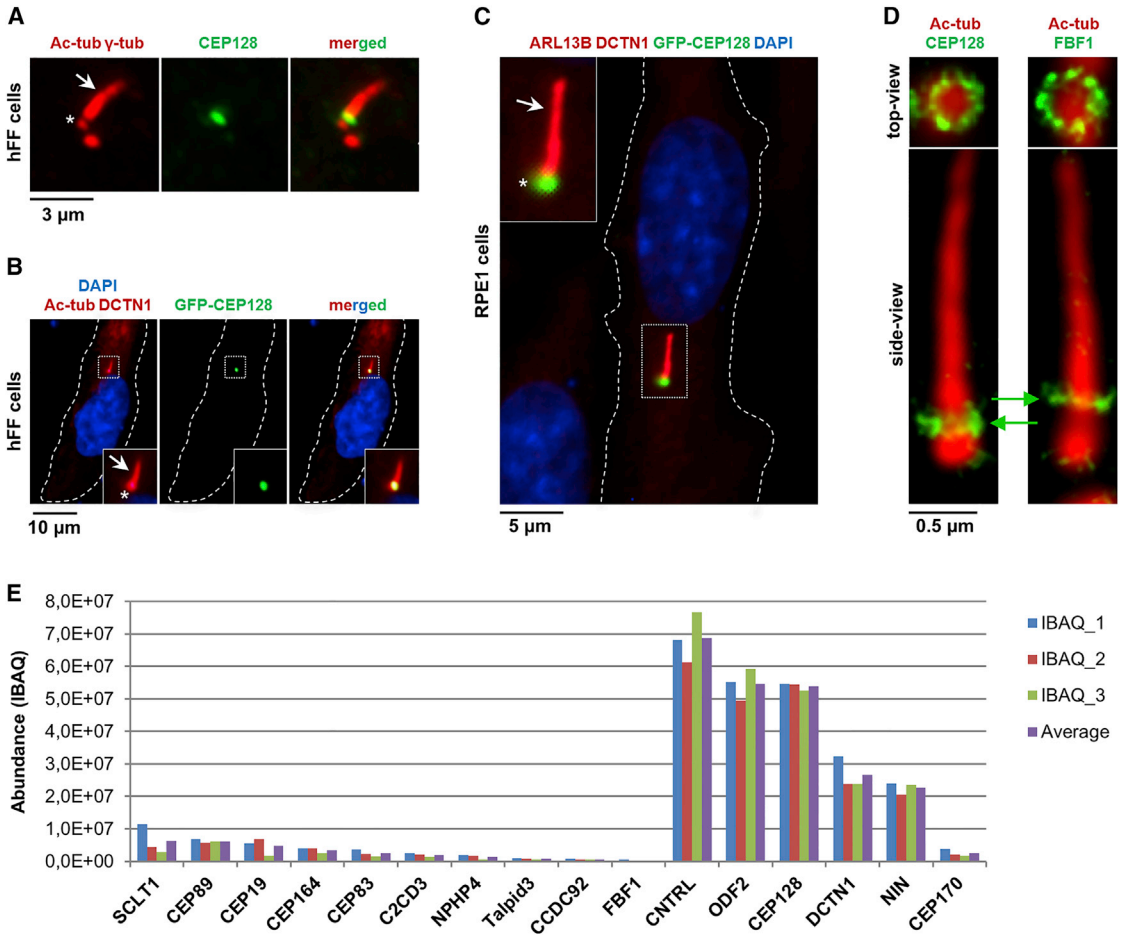

Figure 1. CEP128 Is a Subdistal Appendage Protein

(A–C) IFM of serum-deprived hFF and RPE1 cells using antibodies against acetylated α-tubulin (Ac.tub), ARL13B and γ-tubulin (γ-tub), or DCTN1 to mark the cilium and centrosome (both red), respectively. In (A), endogenous CEP128 was stained using specific antibody. Cells in (B and C) express GFP-CEP128 (green); DNA was stained with 4',6-diamidino-2-phenylindole dihydrochloride (DAPI; blue). Insets: Magnifications of the boxed regions. Asterisks: Basal body. Arrows: Cilium.

(D) IFM of serum-deprived RPE1 cells using STED microscopy. Cells were stained with indicated antibodies. Arrows in the side view images mark the position of the CEP128- and FBF1-containing basal body structures, respectively. Top views suggest centriole-defined substructures with a ninefold symmetry.

(E) Abundance of selected centrosomal proteins estimated from peptide intensity signals from three independent MS analyses of isolated human centrosomes. See also Figures S1 and S2.

revealed that multiple proteins are differentially phosphorylated in TGF-β-stimulated CEP128-deficient cells, including centrosome and MT-associated proteins; molecular motors; RAB11-interacting proteins; and TGF-β/BMP, Hedgehog, mitogen-activated protein kinase (MAPK), tight junction, and focal adhesion signaling components. Immunofluorescence microscopy (IFM) analysis consistently showed that the loss of CEP128 impairs the ciliary activation of SMAD2/3 and recruitment of RAB11, which may account for many of the signaling defects observed in these cells.

RESULTS

CEP128 Is a Subdistal Appendage Protein

We previously showed that CEP128 localizes to the distal end of the mother centriole in non-ciliated human U-2 osteosarcoma cells and to the basal body in ciliated human telomerase-immortalized retinal pigmented epithelial (hTERT-RPE1, hereafter RPE1) cells (Jakobsen et al., 2011). We verified this result by IFM analysis of serum-starved, ciliated human foreskin fibroblasts (hFF) using antibodies against CEP128 and ciliary and centrosomal markers (Figure 1A). Small interfering (si)RNA knockdown and quantification of fluorescence intensity confirmed the specificity of the CEP128 antibody (Figures S1A and S1B), and transiently expressed GFP-CEP128 was similarly concentrated at the basal body in hFF and RPE1 cells (Figures 1B and 1C), substantiating that CEP128 is a mother centriole/basal body-specific protein.

A recent study suggested that CEP128 is a DAP (Gupta et al., 2015), whereas others reported CEP128 to be an SDAP (Hung et al., 2016; Mazo et al., 2016). Using superresolution-stimulated emission depletion (STED) microscopy of ciliated RPE1 cells

stained for endogenous CEP128 or the DAP FBF1 (Wei et al., 2015) and for acetylated α-tubulin to label the axoneme and basal body, we found that CEP128 localizes to the distal end of the basal body in a ring-like pattern proximal to FBF1 and exterior to the centriole wall (Figure 1D). Immunogold electron microscopy (IEM) analysis of thin sections of ciliated hFF cells (Figures S1C and S1D) or isolated centrosomes from non-ciliated KE-37 cells (Figures S1E and S1F) confirmed that CEP128 is an SDAP. Finally, quantitative mass spectrometry (MS) analysis of isolated centrosomes showed that CEP128 cellular abundance is similar to that of known SDAPs (e.g., CNTRL, ODF2), whereas DAPs (e.g., CEP164, FBF1) are less abundant (Figure 1E). We conclude that CEP128 is an SDAP.

CEP128 Negatively Regulates Ciliary Growth

Recently, CEP128 was shown to suppress ciliogenesis in RPE1 cells (Gupta et al., 2015). Another study implicated CEP128 and other SDAPs in keeping primary cilia submerged in a deep membrane pit, which in turn affected signaling (Mazo et al., 2016). However, the precise function of CEP128 remains unclear. We depleted CEP128 from hFF or RPE1 cells by RNA interference (Figures S1A and S1B) and analyzed serum-starved cells by IFM with acetylated α-tubulin antibody, transmission EM (TEM), or both. CEP128-depleted cells displayed cilia and basal bodies that are structurally indistinguishable from those of control cells (Figures S1G–S1I). To support these results, we generated a CEP128 knockout RPE1 cell line (hereafter known as *CEP128*$^{-/-}$) using CRISPR-Cas9 methodology (Figure S1J) and analyzed cells by IFM with antibodies against centrosomal and ciliary markers. Quantification of cilia frequency and length confirmed that cells lacking CEP128 form cilia more readily than do wild-type (WT) cells (Figure S1K) (Gupta et al., 2015) and cilia of *CEP128*$^{-/-}$ cells were longer (Figure S1L). This phenotype was not secondary to cell cycle defects, as revealed by western blot (WB) analysis with antibody against retinoblastoma-associated protein (Rb) phosphorylated at serine 807 and serine 811 (Knudsen and Wang, 1997) (Figure S1M).

Centrosomal localization of CNTRL and CEP128 depends on ODF2 (Tateishi et al., 2013; Hung et al., 2016; Mazo et al., 2016). In contrast, loss of CEP128 neither affected centrosomal localization of ODF2 and CNTRL (Figures S2B, S2D, and S2F) nor of centrosomal or centriolar satellite proteins SSX2IP, PCNT, KIAA0753, AURKA, CEP83, HOOK3, and BBS7 (Figure S2B). The average cellular number of centriolar satellites also was the same in *CEP128*$^{-/-}$ and WT cells (Figures S2C and S2E). Thus, CEP128 loss does not grossly affect centrosome and centriolar satellite composition, which is in line with our TEM data (Figure S1I).

CEP128 Regulates TGF-β/BMP Signaling in Zebrafish and Mammalian Cells

To investigate the physiological relevance of CEP128 function, we used morpholino oligonucleotides (MOs) targeting the translational start site (*cep128* ATG MO) or the splice donor of exon 2 (*cep128* splx MO) to knockdown *cep128* in zebrafish embryos. RT-PCR analysis confirmed that the splx MO significantly reduced splicing; an alternatively spliced product also was affected by the MO (Figure S3A). Both MOs yielded identical phenotypes; specifically, *cep128* morphants displayed a dorsalized phenotype at the 10-somite stage, with mild dorsalization presenting with the embryo not completely surrounding the yolk sac and the tip of the tailbud pointing outward. More severely dorsalized embryos were shorter in stature than the WT and developed mainly on the side of an egg-shaped yolk sac (Figure 2A). The severity of the phenotype increased with the dose of the morpholino (Figure 2B). More important, we could partially rescue the dorsalized phenotype of morphants by co-injection of WT *cep128* mRNA (Figures S3B and S3C). To analyze the dorsalized phenotype further, we performed *in situ* hybridization with dorsoventral markers at an early developmental stage. In *cep128* morphants, the expression areas of the dorsal genes *chd* and *gsc* are increased at the shield stage (12/18 and 11/26 embryos, respectively, Figures 2C and 2D), and at 75% epiboly the expression levels of the ventral gene *eve1* are slightly reduced (6/10 embryos, Figure 2E) compared to WT.

We investigated the morphology of the somites in *cep128* morphants with double *in situ* hybridization, analyzing the expression pattern of *myoD1*, and found that at the 14-somite stage the somites of morphants were thin, elongated, and condensed compared to the WT. The notochord (*ta* expression) was thickened and bent several times (Figure 2G). At a higher MO dose of 0.5 pmol, embryos depleted of Cep128 started dying shortly after the 10-somite stage (data not shown). Surviving morphants at the 22-somite stage showed ectopic and unstructured expression of *ta* in the notochord (Figure 2H). Other organs did not form normally either. At 2dpf, analysis of *myl7* expression revealed an abnormal heart development in *cep128* morphants (Figure S3D), whereas the liver and pancreas were smaller or undetectable in morphants (Figure S3E). It is interesting to note that most of the phenotypes observed in *cep128* morphants are reminiscent of aberrant TGF-β/BMP signaling (Mullins et al., 1996). To investigate this further, we analyzed the expression of dorsoventral markers and TGF-β/BMP pathway genes in *cep128* splx morphants at shield and 75% epiboly stages (Figures S3F and S3G). Several of these genes, including *gsc*, *chd*, *vent*, and *smad7*, were differentially expressed in *cep128* morphants compared to WT, suggesting dysregulated TGF-β/BMP signaling, which is in line with the observed dorsalized phenotype of morphants. To evaluate the effects of Cep128 depletion on BMP-mediated activation of Smad transcription factors, we looked at the phosphorylation levels of Smad1/5/8 via an immunohistochemical analysis of whole-mount embryos. At 75% epiboly there was a slight but significant reduction in the phosphorylation of these transcription factors in morphants (13/34 morphants versus 4/15 WTs; Figure 2F). WB analysis confirmed that morphants display significantly reduced levels of phosphorylated Smad1/5/8 compared to WT (Figures 2I and 2J), and the level of phosphorylated Smad2, which is a downstream target in canonical TGF-β signaling, was similarly reduced in morphants (Figures 2K and 2L). Collectively, the results indicate that Cep128 in zebrafish regulates TGF-β/BMP signaling and, when depleted, causes the dorsalized phenotype and potentially other developmental defects.

To support the zebrafish data and investigate how CEP128 affects TGF-β/BMP signaling in human cells, we performed a

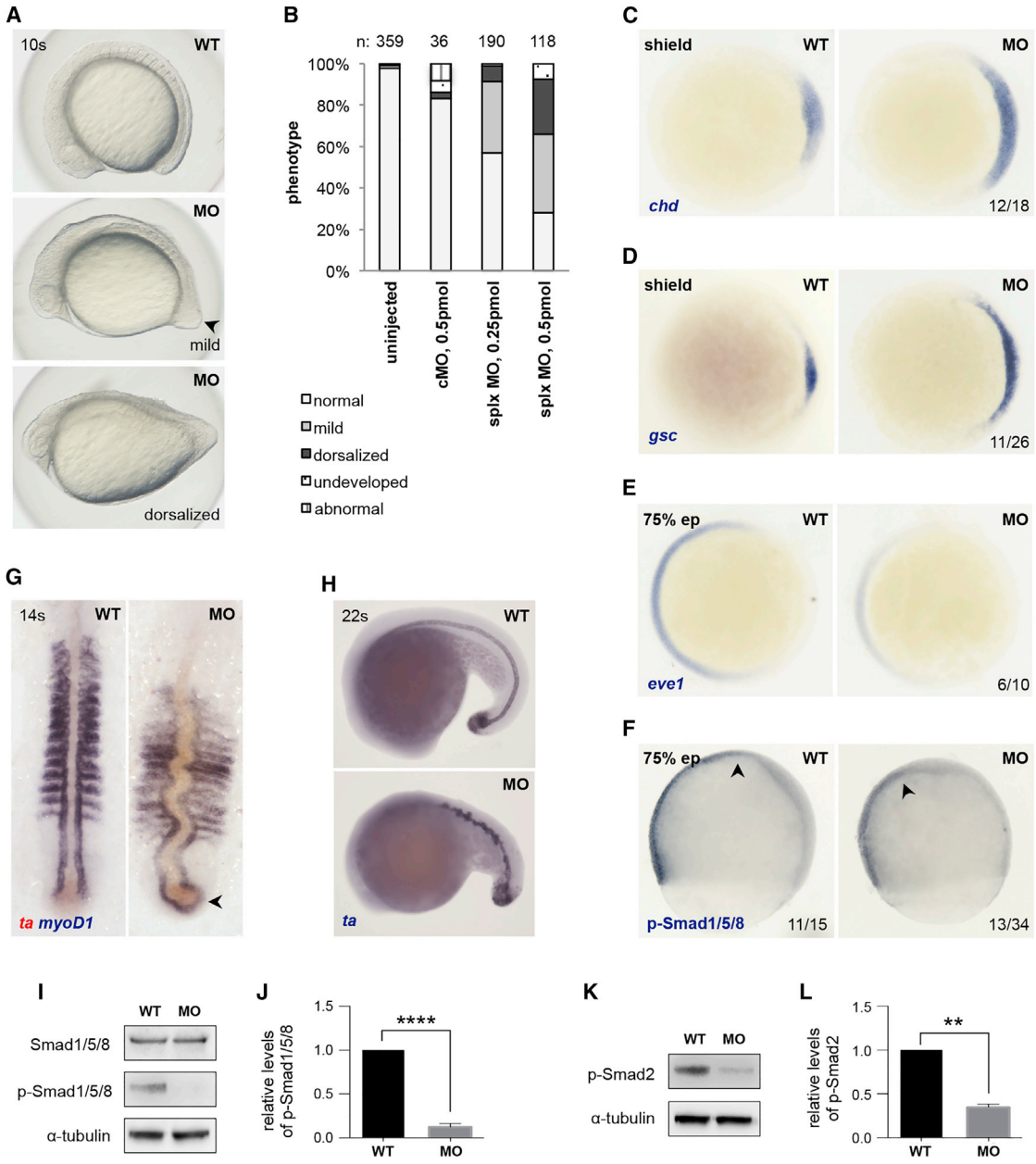

Figure 2. CEP128 Regulates TGF-β/BMP Signaling in Zebrafish

(A) Phenotype of *cep128*-depleted embryos at the 10-somite stage. Embryos show mild (note the pointy tail of the embryo, arrow) to severe (egg-shaped yolk sac) dorsalized morphology. Lateral views, anterior to left.

(B) Numbers for the phenotypic analysis in (A). Two to four independent experiments.

(C–E) Dorsoventral patterning genes are misexpressed in *cep128* splx morphants. Areas of expression of dorsal genes *chd* (C) and *gsc* (D) are increased in morphants; the ventrally expressed gene *eve1* (E) is slightly decreased. Animal pole views, dorsal to right.

(F) The phosphorylation level of Smad1/5/8 is slightly reduced in morphants. The thickened embryonic tissue in the morphants indicates dorsalization of the embryo (arrow). Lateral views, dorsal to right.

(G) *myoD1* expression (blue) shows thin and elongated somites in morphants, with adaxial cells extending around the tail bud (arrowhead); the notochord (*ta* expression, red) is thickened and bent. Dorsal views, anterior to top.

(H) *ta* expression is ectopic and unstructured in the notochord and tailbud areas in *cep128* morphants.

(I–L) WB analysis of embryos at 75% epiboly (I and K) and quantification of relative band intensities (J and L) show that phosphorylation levels of Smad1/5/8 and Smad2 are reduced significantly in morphants compared to WT. Graphs show means ± SDs (n = 3). $^{**}p \leq 0.01$; $^{****}p \leq 0.0001$.

See also Figure S3.

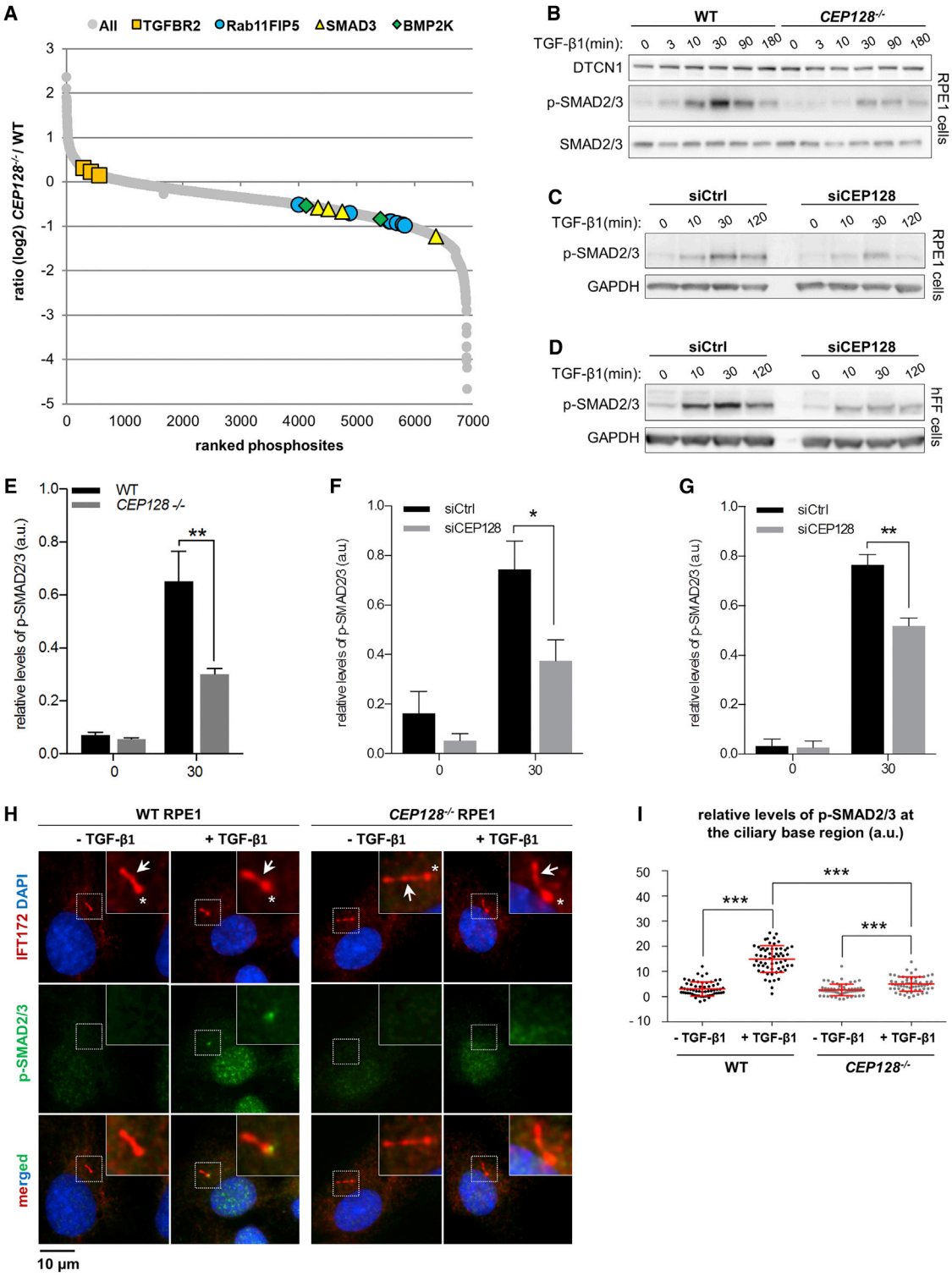

Figure 3. Reduced TGF-β Signaling in Cells Lacking CEP128

(A) TGF-β-induced protein phosphorylation is altered in *CEP128*$^{-/-}$ cells as determined by quantitative MS-based proteomics of phosphopeptides derived from SILAC-labeled cells treated with 2 ng/mL TGF-β1 for 30 min. Phosphopeptides for selected proteins are displayed among all quantified phosphopeptides ranked according to the fold-change (log2 ratio between WT and *CEP128*$^{-/-}$ cells).

(B–D) WB of serum-starved WT and *CEP128*$^{-/-}$ RPE1 cells (B) or RPE1 (C) and hFF (D) cells treated with control (siCtrl) or CEP128-specific (siCEP128) siRNA. Cells were stimulated with 2 ng/mL TGF-β1 for the indicated times. Blots were probed with the indicated antibodies.

(legend continued on next page)

quantitative stable isotope labeling with amino acids in cell culture (SILAC)-based phosphoproteomics experiment to compare the phosphoproteome of WT and *CEP128*$^{-/-}$ RPE1 cells stimulated with TGF-β1. We identified differentially phosphorylated sites in several centrosomal proteins, with CEP170 being the most prominent, as well as in the TGF-β/BMP pathway components SMAD2/3, TAB3, TGFBR2, BMP2K, and BMPR2 (Figure 3A; Table S1). Quantitative WB analysis confirmed that *CEP128*$^{-/-}$ cells exhibit decreased phosphorylation of SMAD2/3 upon TGF-β stimulation compared to WT cells (Figures 3B and 3E), in agreement with the MS data. Similar results were obtained in CEP128 siRNA-depleted RPE1 or hFF cells (Figures 3C, 3D, 3F, and 3G), whereas BMP2-induced phosphorylation of SMAD1/5/8 was less affected by CEP128 loss in these cells (data not shown). Because TGF-β signaling is mediated in part by the primary cilium (Clement et al., 2013), we used IFM to investigate whether CEP128 regulates signaling at the cilium. We found that TGF-β-mediated phosphorylation of SMAD2/3 at the ciliary base is greatly reduced in *CEP128*$^{-/-}$ cells compared to WT cells (Figures 3H and 3I). Thus, CEP128 is required for coordination of TGF-β/BMP signaling in zebrafish and mammalian cells, and CEP128-coordinated signaling is regulated at the primary cilium.

CEP128 Promotes Ciliary Localization of RAB11A

Apart from centrosomal proteins and TGF-β/BMP pathway components, our phosphoproteomic analysis revealed a number of additional differentially phosphorylated proteins in TGF-β-stimulated *CEP128*$^{-/-}$ cells compared to WT cells. Among these were several MT-associated proteins (e.g., MAP1A/1B/2/4/7/9), molecular motors (e.g., kinesin-3 s KIF1B/1C/13A; kinesin-4 s KIF4A/4B/21A/21B/27; cytoplasmic dynein 1/2 subunits DYNC2H1, DYNC1H1, DYNC1I2, and DCTN2), RAB11 interactors (RAB11FIP1/2/5), and RAB8. The most upregulated phosphopeptides were derived mainly from secreted factors such as osteopontin (Table S1).

We subjected the phosphoproteomics data to gene set-enrichment analysis using the log2 transformed phosphopeptide ratios and annotated genes from the Kyoto Encyclopedia of Genes and Genomes (KEGG) pathway database. The enrichment scores indicated that multiple components of major cellular and developmental signaling pathways were enriched among the bottom of the ranked list of downregulated phosphopeptides in *CEP128*$^{-/-}$ cells (Figure 3A). These pathways include TGF-β/BMP, MAPK, Hedgehog, tight junction, and focal adhesion signaling (Table S2). These results suggest a possible role for CEP128 in regulating MT-dependent vesicle trafficking at the cilium in response to TGF-β1 stimulation, which in turn may impinge on TGF-β/BMP signaling as well as additional cross-talking signaling pathways and protein secretion.

Our phosphoproteomics analysis revealed differential phosphorylation of several RAB11-interacting proteins in TGF-β stimulated *CEP128*$^{-/-}$ cells compared to WT. RAB11 regulates TGF-β/BMP receptor trafficking (Mitchell et al., 2004; Deshpande et al., 2016) and ciliary membrane biogenesis (Westlake et al., 2011). We, therefore, tested whether CEP128 affects ciliary recruitment of RAB11. IFM analysis of WT and *CEP128*$^{-/-}$ RPE1 cells revealed that exogenously expressed Myc-RAB11A is highly enriched at the base and along the primary cilium in WT cells but not in *CEP128*$^{-/-}$ cells (Figures 4A–4D). Similar results were obtained in CEP128 siRNA-depleted hFF cells (Figures S4A and S4B). Exogenously expressed GFP-RAB11A^{Q70L}, which mimics GTP-locked RAB11A (Knodler et al., 2010), similarly displays reduced ciliary and centrosomal localization in *CEP128*$^{-/-}$ cells compared to WT cells (Figures 4E and 4F; Figure S4C). The transfected WT and *CEP128*$^{-/-}$ cells displayed similar average expression levels of Myc-RAB11A, whereas *CEP128*$^{-/-}$ cells had a slightly higher average expression level of GFP-RAB11A^{Q70L} than did WT cells (Figure S4D), ruling out that lack of ciliary and centrosomal localization of Myc-RAB11A and GFP-RAB11A^{Q70L} in *CEP128*$^{-/-}$ cells is the result of reduced fusion protein expression. Previous work indicated that RAB11 promotes ciliogenesis by stimulating RABIN8 activity toward RAB8 (Knodler et al., 2010; Westlake et al., 2011). We did not observe any significant difference in endogenous RAB8 ciliary localization in *CEP128*$^{-/-}$ cells compared to WT cells (Figures S4E and S4F), in agreement with *CEP128*$^{-/-}$ cells being ciliated. We conclude that CEP128 promotes ciliary and centrosomal accumulation of RAB11A, which may affect trafficking and regulation of TGF-β/BMP pathway components.

DISCUSSION

We identified CEP128 as a bona fide SDAP with a conserved role in regulating TGF-β/BMP signaling. A recent report indicated that SDAPs (including CEP128) mediate interaction between the centrosome and Golgi, ensuring that cilia become submerged in a pocket-like membrane invagination (Mazo et al., 2016). Although we did not specifically address this phenomenon, our data suggest that a major function of CEP128 *in vivo* is to coordinate TGF-β/BMP signaling and downstream cross-talk with other pathways (e.g., MAPK, Hedgehog, tight junction, focal adhesion signaling) via regulation of ciliary vesicle trafficking. Specifically, in the absence of CEP128, we found that TGF-β induced phosphorylation of multiple RAB11-binding proteins and ciliary/centrosomal recruitment of RAB11A were perturbed. Nevertheless, our results are not in conflict with those of Mazo et al. (2016). Coordination of TGF-β signaling at the primary cilium involves clathrin-mediated endocytosis of TGF-β receptors at the ciliary pocket (Clement et al., 2013),

(E–G) Quantification of relative p-SMAD2/3 levels after 0 and 30 min TGF-β1 stimulation, based on the blots in (B–D), respectively. Relative level of p-SMAD2/3 in WT and *CEP128*$^{-/-}$ RPE1 cells (E), in RPE1 cells treated with control or CEP128-specific siRNA (F), or in hFF cells treated with control or CEP128-specific siRNA (G). Graphs show means ± SDs (n = 4). *p ≤ 0.05; **p ≤ 0.01.

(H) IFM of WT and *CEP128*$^{-/-}$ RPE1 cells ± stimulation with 2 ng/mL TGF-β1 for 30 min. Cells were analyzed with the indicated antibodies, and nuclei were stained with DAPI (blue). Asterisks: Ciliary base. Arrows: Cilium.

(I) Quantification of the data in (H). Graphs show means ± SDs (n = 3). ***p ≤ 0.001. GAPDH, glyceraldehyde-3-phosphate dehydrogenase.

See also Tables S1 and S2.

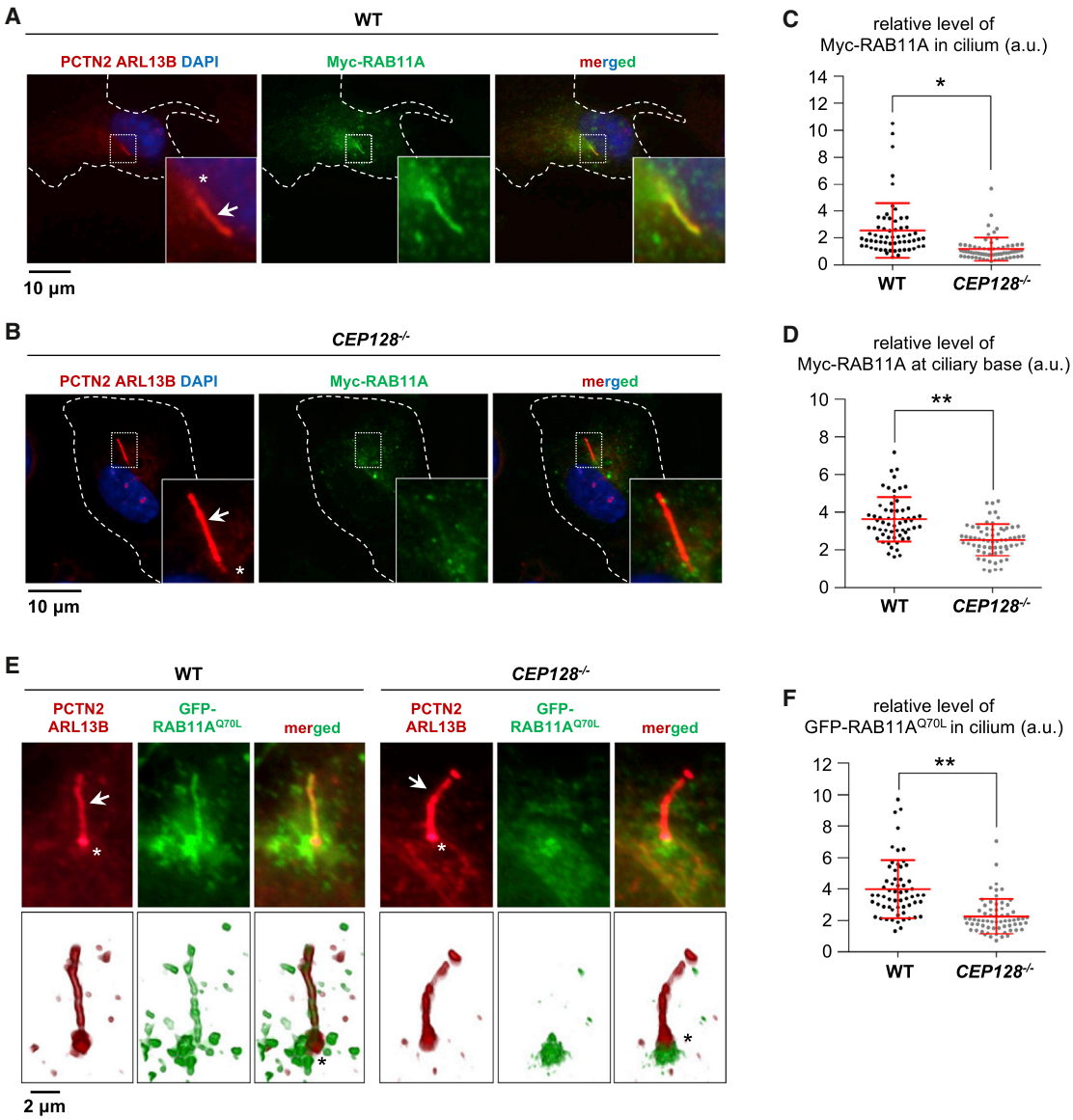

Figure 4. CEP128 Regulates Ciliary and Centrosomal Localization of RAB11

(A and B) IFM analysis of serum-starved WT (A) and *CEP128*$^{-/-}$ (B) RPE1 cells expressing Myc-RAB11A (green). Cells were stained with PCTN1 and ARL13B antibodies (red); DNA was stained with DAPI (blue). Insets: Magnifications of the boxed regions. Asterisks: Ciliary base. Arrows: Cilium.

(C and D) Quantification of the data in (A and B). Relative level of Myc-RAB11A in cilium (C) and relative level of Myc-RAB11A at ciliary base (D). Graphs show means ± SDs (n = 3). *p ≤ 0.05; **p ≤ 0.01.

(E) IFM of serum-starved WT and *CEP128*$^{-/-}$ cells expressing GFP-RAB11A^{Q70L} (green). Cells were stained with PCTN1 and ARL13B antibodies (red). Lower panels show isosurface 3D visualization of the images in the upper panels. Asterisks: Ciliary base. Arrows: Cilium.

(F) Quantification of the data in (E); relative level of GFP-RAB11A^{Q70L} in cilium. Graphs show means ± SDs (n = 3). **p ≤ 0.01.

See also Figure S4.

and if CEP128 is required for ciliary pocket formation (Mazo et al., 2016), then this process may be defective. Our results also do not exclude that some of the *cep128* morphant phenotypes are the result of defects in other ciliary pathways (e.g., Hedgehog signaling).

The SDAPs cenexin and CNTRL were previously shown to mediate centrosomal recruitment and regulation of RAB11, the RAB11 guanosine triphosphatase (GTPase)-activating protein EVI5, and the exocyst complex (Hehnly et al., 2012; Hung et al., 2016). Specifically, it was proposed that GTP-RAB11 associates with SDAPs via cenexin and that CNTRL-associated EVI5 in turn regulates negatively the activity of cenexin-associated RAB11 (Hehnly et al., 2012). Along with the work presented here, these reports substantiate that appropriate regulation of RAB11 at the cilium/centrosome critically relies on SDAPs. Given that RAB11 promotes ciliogenesis by stimulating RABIN8 activity toward

RAB8 (Knodler et al., 2010; Westlake et al., 2011), it is surprising that RAB8 was localized to cilia in *CEP128*$^{-/-}$ cells. Perhaps low levels of RAB11 present at the ciliary base in these cells are sufficient to activate RABIN8/RAB8 and drive ciliogenesis, or other RAB proteins may compensate for the absence of RAB11 in this context, as suggested by other researchers (Sato et al., 2014; Ying et al., 2016). Because RAB11 regulates TGF-β/BMP receptor trafficking (Mitchell et al., 2004; Deshpande et al., 2016), the signaling defects observed upon CEP128 loss may be the result of impaired RAB11-dependent ciliary recruitment of these receptors. It will be important to address this in future studies.

EXPERIMENTAL PROCEDURES

Mammalian Cell Culture and Transfection

RPE1 cells were grown in DMEM, hFF cells were grown in Iscove's Modified Dulbecco's Medium (IMDM) plus GlutaMAX, and KE-67 cells were grown in RPMI 1640 medium. All media were supplemented with 10% fetal bovine serum (FBS) and 1% penicillin-streptomycin. Cells for IFM were grown on glass coverslips in 9.5-cm^2 6-well plates (CellStar); cells for WB were grown in 6-cm diameter Petri dishes.

SDS-PAGE and WB

SDS-PAGE and WB were executed as described (Schrøder et al., 2011) using horseradish peroxidase-conjugated secondary antibodies; blots were developed with FUSION-Fx chemiluminescence system (Vilber Lourmat). Images were processed in Adobe Photoshop CS6 and quantification conducted using ImageJ.

Fluorescence and EM

IFM and TEM analyses of mammalian cells were conducted essentially as described (Schrøder et al., 2011). Quantification of fluorescence intensity and cilia length was carried out using CellSense software (Olympus). The procedures for IEM have been described previously (Geimer, 2009).

Statistical Analysis

The statistical analysis was undertaken in GraphPad Prism 6 by unpaired two-tailed t test or two-way ANOVA followed by Sidak's multiple comparisons.

MS

Control WT and *CEP128*$^{-/-}$ RPE1 cells were SILAC labeled and stimulated with 2 ng/mL TGF-β1 for 30 min before protein digestion with trypsin, high pH peptide separation, and TiO_2-based phosphopeptide enrichment. Following data acquisition by liquid chromatography (LC)-MS, phosphopeptides were identified and quantified using MaxQuant (Cox and Mann, 2008).

Zebrafish

The zebrafish (*Danio rerio*) lines AB, Tüpfel long fin (TL), and ABTL crosses were maintained in the animal facility of the University of Copenhagen. All zebrafish research was approved by and conducted under licenses from the Danish Animal Experiments Inspectorate. Primers used for PCR and cloning are listed in Tables S3 and S4. See Supplemental Information for Supplemental Experimental Procedures and Supplemental References.

SUPPLEMENTAL INFORMATION

Supplemental Information includes Supplemental Experimental Procedures, four figures, and four tables and can be found with this article online at https://doi.org/10.1016/j.celrep.2018.02.043.

ACKNOWLEDGMENTS

This work was supported by grants from the Danish Council for Independent Research (#09-070398, #10-085373, #1331-00254, and #6108-00457B), the Lundbeck Foundation (R209-2015-2604), the Novo Nordisk Foundation (NNF14OC0011535 and NNF15OC0016886), and the University of Copenhagen (UCPH) Excellence Programme for Interdisciplinary Research. We thank M.S. Holm, S.L. Johansen, and L.E. Rasmussen for technical assistance; K. Koefoed and S.K. Morthorst for participation in initial phases of this study; and Johan Peränen, University of Helsinki, for reagents. We are grateful to the Cell Profiling and Advanced Light Microscopy Facility at Science for Life Laboratory, Sweden, for IFM experiments, and the Wallenberg Foundation for funding the Human Protein Atlas generation of antibodies.

AUTHOR CONTRIBUTIONS

M.M. and C.D. conducted the zebrafish studies. L. Borgeskov performed the cell-based assays and the WB and IFM analysis in mammalian cells with assistance from J.B.M., L. Blinkenkjær, and J.M.S. L. Breslin generated *CEP128*$^{-/-}$ cells and did IFM analysis with centrosome and satellite markers. L.J. purified centrosomes and conducted the STED and proteomics analyses with help from E.L., J.S.A., L. Breslin, and L.M.H. M.R., J.M.S., and S.G. performed the EM analyses. All of the authors helped with the data analysis and figure preparation. J.S.A., L.A.L., S.T.C., and L.B.P. conceived the project, designed the experiments, and obtained funding for the study. L.B.P., M.M., and J.S.A. wrote the paper with input from all of the authors.

DECLARATION OF INTERESTS

The authors declare no competing interests.

Received: June 23, 2017
Revised: December 4, 2017
Accepted: February 8, 2018
Published: March 6, 2018

REFERENCES

Clare, D.K., Magescas, J., Piolot, T., Dumoux, M., Vesque, C., Pichard, E., Dang, T., Duvauchelle, B., Poirier, F., and Delacour, D. (2014). Basal foot MTOC organizes pillar MTs required for coordination of beating cilia. Nat. Commun. *5*, 4888.

Clement, C.A., Ajbro, K.D., Koefoed, K., Vestergaard, M.L., Veland, I.R., Henriques De Jesus, M.P.R., Pedersen, L.B., Benmerah, A., Andersen, C.Y., Larsen, L.A., and Christensen, S.T. (2013). TGFβ signaling is associated with endocytosis at the pocket region of the primary cilium. Cell Rep. *3*, 1806–1814.

Cox, J., and Mann, M. (2008). MaxQuant enables high peptide identification rates, individualized p.p.b.-range mass accuracies and proteome-wide protein quantification. Nat. Biotechnol. *26*, 1367–1372.

Deane, J.A., Cole, D.G., Seeley, E.S., Diener, D.R., and Rosenbaum, J.L. (2001). Localization of intraflagellar transport protein IFT52 identifies basal body transitional fibers as the docking site for IFT particles. Curr. Biol. *11*, 1586–1590.

Deshpande, M., Feiger, Z., Shilton, A.K., Luo, C.C., Silverman, E., and Rodal, A.A. (2016). Role of BMP receptor traffic in synaptic growth defects in an ALS model. Mol. Biol. Cell *27*, 2898–2910.

Geimer, S. (2009). Immunogold labeling of flagellar components in situ. Methods Cell Biol. *91*, 63–80.

Graser, S., Stierhof, Y.D., Lavoie, S.B., Gassner, O.S., Lamla, S., Le Clech, M., and Nigg, E.A. (2007). Cep164, a novel centriole appendage protein required for primary cilium formation. J. Cell Biol. *179*, 321–330.

Gromley, A., Yeaman, C., Rosa, J., Redick, S., Chen, C.T., Mirabelle, S., Guha, M., Sillibourne, J., and Doxsey, S.J. (2005). Centriolin anchoring of exocyst and SNARE complexes at the midbody is required for secretory-vesicle-mediated abscission. Cell *123*, 75–87.

Guarguaglini, G., Duncan, P.I., Stierhof, Y.D., Holmstrom, T., Duensing, S., and Nigg, E.A. (2005). The forkhead-associated domain protein Cep170 interacts with Polo-like kinase 1 and serves as a marker for mature centrioles. Mol. Biol. Cell *16*, 1095–1107.

Gupta, G.D., Coyaud, E., Goncalves, J., Mojarad, B.A., Liu, Y., Wu, Q., Gheiratmand, L., Comartin, D., Tkach, J.M., Cheung, S.W., et al. (2015). A Dynamic Protein Interaction Landscape of the Human Centrosome-Cilium Interface. Cell *163*, 1484–1499.

Hehnly, H., Chen, C.T., Powers, C.M., Liu, H.L., and Doxsey, S. (2012). The centrosome regulates the Rab11-dependent recycling endosome pathway at appendages of the mother centriole. Curr. Biol. *22*, 1944–1950.

Huangfu, D., Liu, A., Rakeman, A.S., Murcia, N.S., Niswander, L., and Anderson, K.V. (2003). Hedgehog signalling in the mouse requires intraflagellar transport proteins. Nature *426*, 83–87.

Hung, H.F., Hehnly, H., and Doxsey, S. (2016). The Mother Centriole Appendage Protein Cenexin Modulates Lumen Formation through Spindle Orientation. Curr. Biol. *26*, 1248.

Jakobsen, L., Vanselow, K., Skogs, M., Toyoda, Y., Lundberg, E., Poser, I., Falkenby, L.G., Bennetzen, M., Westendorf, J., Nigg, E.A., et al. (2011). Novel asymmetrically localizing components of human centrosomes identified by complementary proteomics methods. EMBO J. *30*, 1520–1535.

Jensen, V.L., and Leroux, M.R. (2017). Gates for soluble and membrane proteins, and two trafficking systems (IFT and LIFT), establish a dynamic ciliary signaling compartment. Curr. Opin. Cell Biol. *47*, 83–91.

Kenny, T.D., and Beales, P.L. (2014). Ciliopathies: A Reference for Clinicians (Oxford University Press).

Knodler, A., Feng, S., Zhang, J., Zhang, X., Das, A., Peranen, J., and Guo, W. (2010). Coordination of Rab8 and Rab11 in primary ciliogenesis. Proc. Natl. Acad. Sci. USA *107*, 6346–6351.

Knudsen, E.S., and Wang, J.Y. (1997). Dual mechanisms for the inhibition of E2F binding to RB by cyclin-dependent kinase-mediated RB phosphorylation. Mol. Cell. Biol. *17*, 5771–5783.

Kunimoto, K., Yamazaki, Y., Nishida, T., Shinohara, K., Ishikawa, H., Hasegawa, T., Okanoue, T., Hamada, H., Noda, T., Tamura, A., et al. (2012). Coordinated ciliary beating requires Odf2-mediated polarization of basal bodies via basal feet. Cell *148*, 189–200.

Mazo, G., Soplop, N., Wang, W.J., Uryu, K., and Tsou, M.B. (2016). Spatial Control of Primary Ciliogenesis by Subdistal Appendages Alters Sensation-Associated Properties of Cilia. Dev. Cell *39*, 424–437.

Mitchell, H., Choudhury, A., Pagano, R.E., and Leof, E.B. (2004). Ligand-dependent and -independent transforming growth factor-beta receptor recycling regulated by clathrin-mediated endocytosis and Rab11. Mol. Biol. Cell *15*, 4166–4178.

Mogensen, M.M., Malik, A., Piel, M., Bouckson-Castaing, V., and Bornens, M. (2000). Microtubule minus-end anchorage at centrosomal and non-centrosomal sites: the role of ninein. J. Cell Sci. *113*, 3013–3023.

Mullins, M.C., Hammerschmidt, M., Kane, D.A., Odenthal, J., Brand, M., Van Eeden, F.J., Furutani-Seiki, M., Granato, M., Haffter, P., Heisenberg, C.P., et al. (1996). Genes establishing dorsoventral pattern formation in the zebrafish embryo: the ventral specifying genes. Development *123*, 81–93.

Sato, T., Iwano, T., Kunii, M., Matsuda, S., Mizuguchi, R., Jung, Y., Hagiwara, H., Yoshihara, Y., Yuzaki, M., Harada, R., and Harada, A. (2014). Rab8a and Rab8b are essential for several apical transport pathways but insufficient for ciliogenesis. J. Cell Sci. *127*, 422–431.

Schrøder, J.M., Larsen, J., Komarova, Y., Akhmanova, A., Thorsteinsson, R.I., Grigoriev, I., Manguso, R., Christensen, S.T., Pedersen, S.F., Geimer, S., and Pedersen, L.B. (2011). EB1 and EB3 promote cilia biogenesis by several centrosome-related mechanisms. J. Cell Sci. *124*, 2539–2551.

Sorokin, S. (1962). Centrioles and the formation of rudimentary cilia by fibroblasts and smooth muscle cells. J. Cell Biol. *15*, 363–377.

Taschner, M., and Lorentzen, E. (2016). The Intraflagellar Transport Machinery. Cold Spring Harb. Perspect. Biol. *8*, a028092.

Tateishi, K., Yamazaki, Y., Nishida, T., Watanabe, S., Kunimoto, K., Ishikawa, H., and Tsukita, S. (2013). Two appendages homologous between basal bodies and centrioles are formed using distinct Odf2 domains. J. Cell Biol. *203*, 417–425.

Veleri, S., Manjunath, S.H., Fariss, R.N., May-Simera, H., Brooks, M., Foskett, T.A., Gao, C., Longo, T.A., Liu, P., Nagashima, K., et al. (2014). Ciliopathy-associated gene Cc2d2a promotes assembly of subdistal appendages on the mother centriole during cilia biogenesis. Nat. Commun. *5*, 4207.

Wei, Q., Ling, K., and Hu, J. (2015). The essential roles of transition fibers in the context of cilia. Curr. Opin. Cell Biol. *35*, 98–105.

Westlake, C.J., Baye, L.M., Nachury, M.V., Wright, K.J., Ervin, K.E., Phu, L., Chalouni, C., Beck, J.S., Kirkpatrick, D.S., Slusarski, D.C., et al. (2011). Primary cilia membrane assembly is initiated by Rab11 and transport protein particle II (TRAPPII) complex-dependent trafficking of Rabin8 to the centrosome. Proc. Natl. Acad. Sci. USA *108*, 2759–2764.

Ying, G., Gerstner, C.D., Frederick, J.M., Boye, S.L., Hauswirth, W.W., and Baehr, W. (2016). Small GTPases Rab8a and Rab11a Are Dispensable for Rhodopsin Transport in Mouse Photoreceptors. PLoS One *11*, e0161236.